Study on the combustion indices of forest species using thermogravimetric analysis

Yassine Rahib[1,2] · Valérie Leroy-Cancellieri[1] · Dominique Cancellieri[1] · Jacky Fayad[1] · Jean-Louis Rossi[1] · Eric Leoni[1]
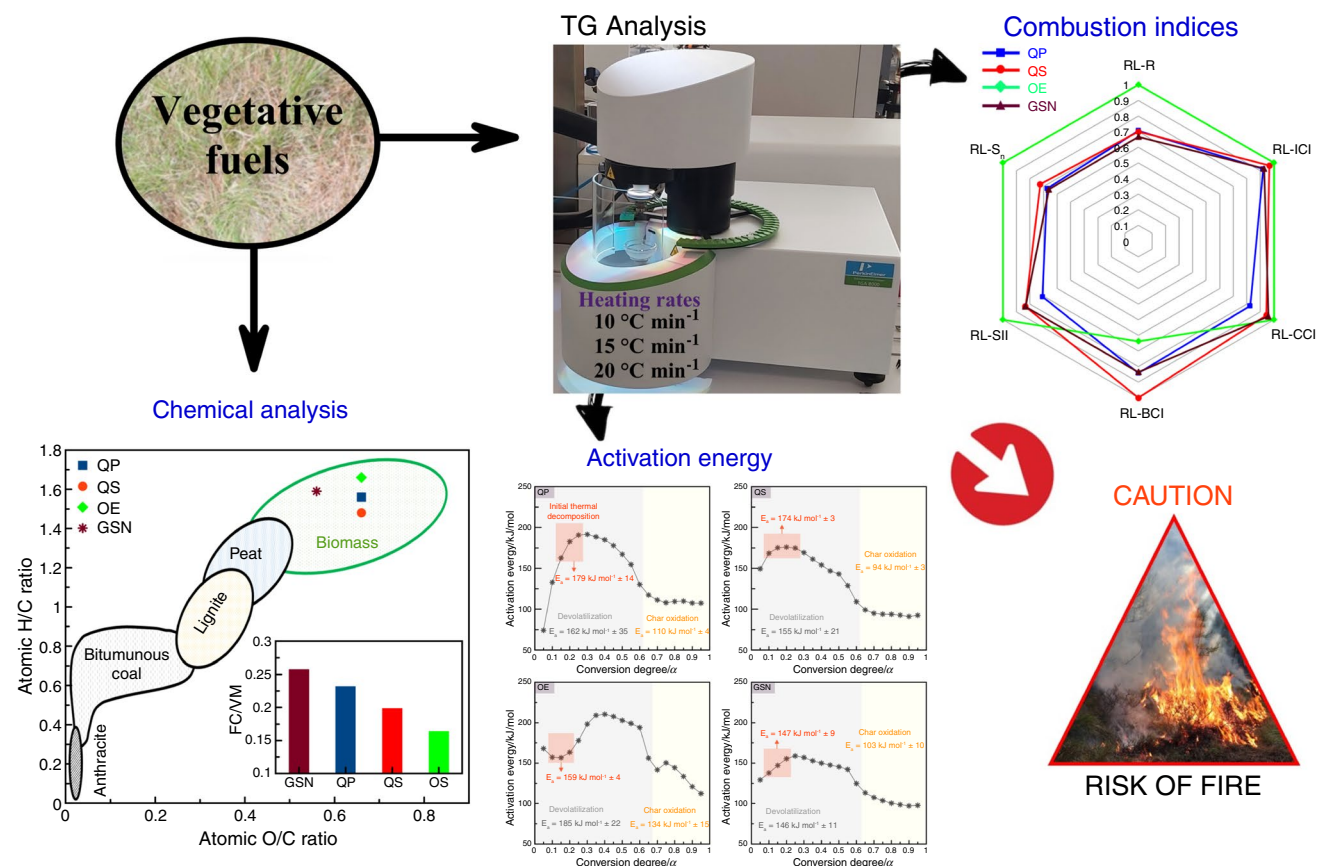
Abstract

The challenges of this work focus on better understanding combustion characteristics and their importance to fire hazard by performing thermogravimetric analysis (TGA). The ultimate goal is to provide a methodology for determining the most relevant indices for a robust fire hazard classification of the species. One of the principles of this methodology is the use of a linear regression method for determining the indices and the activation energy. To achieve this scope, chemical, thermal and kinetic analysis will be performed. Nine combustion indices were calculated and compared to assess combustion characteristics such as ignition, combustion and burnout. Experiments were carried out at three heating rates of 10, 15 and 20 °C min^{-1} under air atmosphere. A selection of forest materials frequently devastated by wildfire, i.e., *Quercus pubescens* (QP), *Quercus suber* (QS), *Olea europaea* (OE) and *Genista Salzmannii* needles (GSN), were studied. The TG-DTG curves have shown that the combustion process consists of two stages: devolatilization and char oxidation. The whole process was controlled by the release of volatile gases. According to the relative linearized (RL) index of spontaneous ignition, the samples were ordered as follows: OE > GSN ≥ QS > QP. OE appears to be the most reactive and prone to spontaneous ignition compared to the other samples. The same order was achieved for the combustion characteristic index and, approximately, for the integrated flammability. On the other hand, the average E_a at the low temperature stage of the combustion process was low for GSN (147 ± 9 kJ mol^{-1}) and OE (159 ± 4 kJ mol^{-1}) and high for QP (179 ± 14 kJ mol^{-1}) and QS (174 ± 3 kJ mol^{-1}). Finally, this work provides valuable insight into the relationship between chemical properties and combustion indices and the components that make some indices more effective than others.

✉ Yassine Rahib
  yassine.rahib@epf.fr; rahib_y@univ-corse.fr

1 SPE Laboratory, UMR-CNRS 6134, Campus Grimaldi, University of Corsica, BP 52, 20250 Corte, France

2 EPF School of Engineering, 2 rue Fernand Sastre, 10430 Rosières-Prés-Troyes, France

Graphical abstract

Abbreviations

BCI	Burnout characteristic index (% min^{-4})
C	Flammability (% min^{-1} °C^{-2})
CCI	Combustion characteristic index (1 min^{-2} °C^{-3})
CSI	Combustion stability index (% min^{-1} °C^{-2})
DI$_{com}$	Devolatilization index for combustion (1 min^{-1} °C^{-2})
DDTG	Second derivative mass loss (% min^{-2})
DTG	Derivative of thermogravimetry (% min^{-1})
DTG$_{max}$	Maximum combustion rate (% min^{-1})
DTG$_{mean}$	Mean combustion rate (% min^{-1})
DTG$_{shoulder}$	Combustion rate of shoulder (% min^{-1})
DTG$_{peak}$	Combustion rate of peak (% min^{-1})
E$_a$	Apparent activation energy (kJ mol^{-1})
FC	Fixed carbon (mass%)
FWO	Flynn–Wall–Ozawa
GSN	*Genista Salzmannii DC.* Needles
HHV	High heating value (MJ kg^{-1})
ICI	Ignition characteristic index (% min^{-3})
ICTAC	International confederation for thermal analysis and calorimetry
KAS	Kissinger–Akahira–Sunose
LHV	Low heating value (MJ kg^{-1})
M	Mass loss in each stage
OE	*Olea europaea L.*
QP	*Quercus pubescens Willd*
QS	*Quercus suber L.*
R	Reactivity (% min^{-1} °C^{-1})
R$_{devolatilization}$	Reactivity during devolatilization stage (% min^{-1} °C^{-1})
R$_{char oxidation}$	Reactivity during char oxidation stage (% min^{-1} °C^{-1})
RL indices	Relative linearized indices
S$_i$	Index of flammability in the stage i
SII	Spontaneous ignition index
S$_n$	Integrated flammability
TGA or TG	Thermogravimetric analysis
T$_b$	Burnout temperature (°C)
t$_b$	Corresponding time of T$_b$ (min)

T_{DTGmax}	Corresponding temperature of DTG_{max} (°C)
t_{DTGmax}	Corresponding time of DTG_{max} (min)
T_{pi}	Pyrolysis initiation temperature (°C)
t_{pi}	Pyrolysis initiation time (min)
T_{peak}	Peak temperature (°C)
TR	Temperature range
T_{shoulder}	Shoulder temperature (°C)
T_{υ}	Initial temperature of volatile release (°C)
t_{υ}	Corresponding time of T_{υ} (min)
VM	Volatile matter (mass%)
α	Conversion degree
β	Heating rate (°C min⁻¹)
$\Delta T_{1/2}$	Temperature range at the half value of DTG_{max} (°C)
$\Delta t_{1/2}$	Time range at the half value of DTG_{max} (min)

Introduction

Over the last decade, climate change has increased global temperatures and caused severe and prolonged droughts, creating an environment that is more prone to wildfires [1, 2]. Forest fires are recognized as an important source of air pollutants with multiple impacts on the environment (global carbon balance, forest wildlife, biodiversity, and ecosystems), economic activity and people's health at local, regional and global levels. Fires start and spread due to three main factors that form the fire triangle: vegetative fuel, weather conditions, and topography [3]. Given the complex interplay of these factors, the only effective action that can be managed seems to be related to vegetation. This may explain the strategies developed to decrease fuel loads in forests to mitigate fire hazards and reduce costs of fuel reduction treatments by including biomass energy removal options [4, 5]. However, the ability to quantify the fire characteristics of vegetative fuels, including fire risk and fire behavior, is still limited. This is in part due to great variations in fire behavior, involving both chemical reactions and physical processes, in different plant populations. The burning of plant species during wildfires entails a series of complex processes. It begins with dehydration and oxidative pyrolysis, with the release and ignition of combustible gases, followed by oxidation of the char formed, and ends with residual combustion and ash formation. Moreover, the high thermal reactivity of plant-based fuels at low temperatures can result in self-ignition problems, requiring extra safety measures [6]. Consequently, the thermal decomposition behavior of natural fuels is important to understand the spread and management of forest fires.

Thermoanalytical techniques (TG-DTG) play an important role in the evaluation of vegetative fuels by determining combustion characteristics and kinetic parameters that are important to explain the ongoing processes [7, 8]. In the field of renewable energy sources, several studies have investigated the combustion behavior and performance of biomass materials using the TG-DTG method. They use many characteristic indices of reactivity, ignitability, flammability, combustibility and burnout [9–16]. In wildfire situations, combustion characteristics can also help guide the safe management and fire protection of these species. Some articles have used TG-DTG to classify plant species according to their index of combustion. For instance, Zhang et al. [17] calculated the flammability index of common grassland species and categorized them based on their ignitability, combustibility and sustainability. Anderson [18] and Liodakis and Kakardakis [19] also investigated the flammability index of forest species. Xie et al. [20] studied the fire hazard levels of three straw powders by TGA and cone calorimetry. The two systems present the same classification of the biomass studied according to the risk assessment. Manic et al. [21] proposed a method for assessing the self-ignition trend of biomass materials. The authors developed a thermogravimetric spontaneous combustion index based on TG-DTG results with slow heating rates. Kumar Mohalik et al. [22] used thermogravimetric and differential scanning calorimeter (TGA and DSC) techniques and physicochemical characterization to determine the spontaneous combustion behavior of coal. The authors suggest four classification groups in accordance with the susceptibility to spontaneous combustion. Generally, literature research focuses on one specific index, phenomenon or process (i.e., flammability or ignition), but to our knowledge, no study has identified relevant indices and suggested their use for planning purposes against forest fire risk.

With respect to kinetic analysis, the activation energy (E_a) represents the smallest amount of energy required to undergo a specific chemical reaction. This is a very important parameter to evaluate the potential for spontaneous combustion of different types of solid fuels. Shu et al. [23] used TGA to study the thermal decomposition kinetics of various forest waste fuels. The authors evaluate the combustibility potential of dead-surface fuels based on the ignition index and activation energy values. Liu et al. [24] investigated the characteristics and kinetics of the pyrolysis and combustion of three biomasses. The authors found that the results from the auto-ignition experiments matched the activation energy and the comprehensive combustion index results. García Torrent et al. [25] examined the impact of biomass composition on susceptibility to spontaneous combustion. They used a hazard diagram based on activation energy and typical temperatures to classify the spontaneous combustion of biomass materials. Other studies have also used TGA and DSC to characterize combustion processes and kinetics and link them to flammability and fire resistance [26, 27].

To date, research in the literature shows that the relationship between the chemical composition of the fuel, combustion characteristics, and kinetics has not been well investigated. Few researchers have used activation energy data to discuss the self-ignition propensity of plant species. In addition, the combustion indices have been partially studied to support fire research and landscape management, and thus, they require optimization to be considered for forest fire management.

The aim of this study is to propose a new method, including a set of relevant indices and factors, for a reliable classification of forest fuels toward wildland fire risk. So, the thermal decomposition behavior of four forest materials was studied by using TGA under an oxidative atmosphere at 10, 15 and 20 °C min^{-1}. Moreover, a comprehensive set of combustion characteristic indices were calculated for the three heating rates. A comparison study was provided in order to evaluate the spontaneous combustion propensity of the materials tested. Furthermore, a model-free method (KAS) was used to estimate the apparent activation energy. Overall, this study provides valuable insights into the factors affecting the wildland fire risk of biomass fuels. The comprehensive set of combustion characteristic indices calculated in this study can help in the reliable classification of biomass fuels. The comparison study and use of model-free methods also enhance the accuracy and reliability of the findings.

Materials and methods

Test samples

Four vegetative fuels were used in this work: *Quercus pubescens* Willd (IPNI[1]: 326,376–2)-QP-, *Quercus suber L.* (IPNI: 297,685–1) -QS-, *Olea europaea L.* (IPNI: 610,675–1) -OE-, and *Genista salzmannii DC.* (IPNI: 496,324–1) -GSN-. These species were selected for various reasons. First, they are very widely distributed in the Mediterranean region, which is recognized as a forest fire danger zone. Additionally, Genista salzmannii L. was recently point out to cause high-intensity fires when exposed to fire in field-scale experiments [28]. Finally, two types of Quercus were selected to see if the method is sensitive enough for similar plant species. Samples were collected in different mountain forests of Corsica (France) in the areas of Letia (42°11′39.84"N/8°52′23.19"E), Corte (42°17′8.01"N/9° 9′20.87"E) and Lucciana (42°32′49.67"N/ 9°24′54.08"E). Fig. S1 in the supplementary section shows the sampling points on the map of Corsica. Once the materials were obtained, leaves and twigs or needles smaller than 2 mm

in diameter were selected from each species. Each sample was oven dried at 60 °C for approximately 24 h, crushed (by using a Lab mill model PX-MFC 90 D) and sieved to get a particle size of less than 100 μm. The final samples were obtained from well-mixed and homogenized leaves and twigs (or needles in case of GSN) and stored in plastic tubes for analysis.

Proximate and ultimate analysis

Proximate analysis was carried out according to the procedure outlined in our previous study [29]. The ultimate analysis (total content of C, H, N, S and O) was performed by the Aix-Marseille University Spectropole using a Flash EA 1112 series Thermo-Finnigan analyzer. Each experiment was carried out at least twice. After the experiments, the fuel ratio (FC/VM) and the O/C and H/C ratios were calculated for all samples. Moreover, the energy content (HHV and LHV) was calculated using the methodology described in reference [30].

TG analysis

The combustion experiments were performed using a PerkinElmer TGA 8000 analyzer with an accuracy of 0.001 mg. Sample mass loss was measured as a function of temperature by the Pyris software manager. The TG analyzer was calibrated for mass loss, temperature, and sensitivity before experimentation. Sample temperature, which is monitored by a thermocouple, did not show any systematic deviation from the preset linear temperature programs. In each experiment, milled samples weighing around 5 ± 0.2 mg were placed in a ceramic crucible and heated (with an accuracy of ± 2 °C) from room temperature to 1000 °C until no further mass change was observed. The combustion atmosphere was air with a flow rate of 30 mL min^{-1}. A low mass and particle size of less than 100 μm for each sample was chosen to eliminate the effects of side reactions and mitigate heat and mass transfer limitations [14, 31]. In general, the properties of the TG-DTG (that is, the peak/shoulder temperature and the maximum mass loss rate) are affected by changes in heating rate, particularly during the devolatilization stage [9, 13]. Otherwise, in our previous study [32], the calculated combustion parameters based on the TG-DTG properties were not affected by particle size changes (crushed versus intact state) at low heating rates (20 °C min^{-1}). For this reason, three slow heating rates of 10, 15 and 20 °C min^{-1} were chosen to distinguish the characteristics of each process and promote homogenous ignition [33]. Finally, the thermal behavior of xylan (from Birch wood), cellulose (microgranular) and lignin (organosolv) provided by Sigma-Aldrich were investigated at a typical heating rate of 15 °C min^{-1} for comparison purposes. All experiments were performed

---

[1] International Plant Name Index.

Combustion characteristic indices

In this work, combustion indices were used to evaluate the ignitability, combustibility, and thermal stability of the samples. The set of selected thermal indices is composed of the following: thermal reactivity (R), ignitability indices (C, DI_{comb} and ICI), combustibility indices (CCI, CSI and BCI), spontaneous combustion index (SII) and the integrated flammability index (S_n). Table 1 lists their definitions, their implications for fire risk and their calculation formulas. All these indices require the knowledge of typical temperature parameters based on the TG-DTG data, including pyrolysis (or oxidative pyrolysis) initiation temperature (T_{pi}), maximum mass loss rate temperature ($T_{DTG\,max}$), burnout temperature (T_b), their corresponding times ($t_{pi}, t_{DTG\,max}$ and t_b), maximum and mean rates of mass loss (DTG_{max} and DTG_{mean}) and temperature and time interval at the half value of DTG_{max} in the descending and the rising part of the peak (ΔT and Δt, respectively).

The procedure for determining these parameters is visualized in Fig. 1. Since ignition in plant species occurs shortly after initial mass loss, T_{pi} was determined by the graphical approach used in the Refs. [42]. A simple change was made in the first stage of the procedure. A vertical line across the first pronounced shoulder (instead of the DTG peak) was created upward to meet the TG oblique line. The second derivative mass loss curve (DDTG) was used to determine the most prominent shoulder position (Fig. 1). This modification was intended to determine the lowest ignition/combustion temperature for the fuel. We consider this to be an improved representation of sensitivity to inflammation. Finally, T_b was defined when the DTG curve reached 0.1%/min after the carbonization reaction [43].

Concerning the assessment of the SII, a simple and fast method was investigated. The approach adopted is based on that of Ref. [21]. From the onset of thermal decomposition to the first DTG peak (usually DTG_{max} during devolatilization), the specific characteristic temperatures identified were T_υ (the initial temperature of volatile releases), T_{pi}, $T_{shoulder}$ (the most prominent shoulder if applicable), and T_{peak}. The T_υ was determined when the mass loss rate reached 0.1%/min after removal of the residual water (Fig. 1). The linear regression between the specific characteristic temperatures and the corresponding DTG values gives a linear equation for each heating rate. The resulting slopes can be considered for a second linear regression as a function of heating rate. A new linear equation can be determined for each sample. The slope of the last equation was considered SII.

Kinetic analysis

Activation energy determination

The kinetics of combustion of solid plant species under non-isothermal conditions can be characterized according to the Arrhenius theory. Using a linear heating rate, the kinetic equation can be expressed as follows:

$$\frac{d\alpha}{dT} = \frac{A_{(\alpha)}}{\beta} e^{\frac{-E_{a(\alpha)}}{R \cdot T}} f(\alpha) \tag{10}$$

where α is the conversion degree ($\alpha = (m_0 - m_t)/(m_0 - m_f)$), T is the absolute temperature (K), β is the heating rate (K min^{-1}), A is the pre-exponential factor, E is the activation energy, R is the ideal gas constant that is defined as 8.314 J mol^{-1}. K and $f(\alpha)$ represent the differential form of the reaction model.

According to the recommendations of the ICTAC [44, 45], the iso-conversional methods provide a better estimate of activation energy. The Kissinger–Akahira–Sunose (KAS) method was developed using the integration and application of the Coats–Redfern approximation. The KAS method is regarded as more accurate for E_α values than the Flynn–Wall–Ozawa (FWO) method due to its better approximation of the temperature integral [44, 46]. The model is based on Eq. (11):

$$\ln\left(\frac{\beta}{T^2}\right) = \ln\left(\frac{A_\alpha \cdot R}{E_{a(\alpha)} \cdot g(\alpha)}\right) - \left(\frac{E_{a(\alpha)}}{R \cdot T}\right) \tag{11}$$

The slope obtained by plotting $\ln(\beta/T^2)$ versus $1/T$ gives the values of activation energy [8].

Numerical method for kinetic validation

A numerical method which allows the calculation of the solid temperature at different conversion degrees was applied to improve the kinetic parameters previously obtained. Leroy et al. [47] has already used this approach in the context of forest fires with similar experimental conditions.

The *Mathematica® Package (Wolfram, 2003): "Solve"* was used in order to provide the explicit formulas for solving the nonlinear Eq. 11. This function gives the complete set of possible solutions (see Eq. 12):

$$T(\alpha) = -\frac{E_{a(\alpha)}/R}{2W\left(\frac{1}{2}\sqrt{\frac{10^b (E_{a(\alpha)})^2/R}{\beta}}\right)} \tag{12}$$

W represents the "product log" function giving the solution for w in $z = we^w$. The function can be viewed as a

Table 1 Mean combustion characteristic indices related to fire risk and management using the TG method

| Index	Equations/methods	Significance for fire risk	References
Reactivity of reaction	$R = 100 * \sum \dfrac{\|DTG_{\text{peak/shoulder}}\|}{T^2_{\text{pi}}}$	(1) Measure the rate of decomposition of structural components specified by the DTG peaks during thermochemical conversion	[34–36]
Flammability index	$C = \dfrac{\|DTG_{\max}\|}{T^2_{\text{pi}}}$	(2) Reflects ignition at the early stage of combustion. Fuels burn easier at higher C	[15, 24, 37]
Devolatilization index for combustion	$DI_{\text{comb}} = \dfrac{\|DTG_{\max}\|}{T_{DTG_{\max}} * (T_{DTG_{\max}} - T_{\text{pi}})}$	(3) Refers to the release of volatile components during combustion	[38]
Ignition characteristic index	$ICI = \dfrac{\|DTG_{\max}\|}{t_{\text{pi}} * t_{DTG_{\max}}}$	(4) This is the ignition performance of fuel combustion. The higher the ICI, the greater the separation of volatile compounds from the fuel, which facilitates early ignition	[9, 20, 38]
Combustion characteristic index	$CCI = \dfrac{\|DTG_{\max}\| * \|DTG_{\text{mean}}\|}{T^2_{\text{pi}} * T_b}$	(5) Preliminary evaluation of flammability (C) and burnout behavior of samples. The higher the CCI, the better the combustion activity and the faster the char burns down	[24, 38–40]
Combustion stability index	$CSI = 8,5875 * 10^7 \dfrac{\|DTG_{\max}\|}{T_{DTG_{\max}} * T_{\text{pi}}}$	(6) Evaluation of the burning stability of the samples. A higher CSI value means a better combustion stability of the sample	[41]
Burnout characteristic index	$BCI = \dfrac{\|DTG_{\max}\|}{\Delta t_{1/2} * t_{DTG_{\max}} * t_b}$	(7) Represents the ability to combust fuels. Unlike ICI, it focuses more on the end of the reaction	[20, 38]
Spontaneous ignition index	SII based on TG-DTG curves: linear interpolation of the characteristic temperatures and heating rates	(8) Check the susceptibility to self-ignition. This index can be used to compare and rank solid fuels in terms of their potential for self-ignition	Inspired from [21]
Integrated flammability index	$S_{1,2,3} = \dfrac{\|DTG_{\max 1,2,3}\| * \|DTG_{\text{mean} 1,2,3}\|}{T^2_{\text{pi} 1,2,3} * T_{DTG_{\max} 1,2,3}}$ $S_n = \dfrac{M_1 S_1 + M_2 S_2 + M_3 S_3}{M_1 + M_2 + M_3}$ 1: first major stage; 2: second major stage; 3: third major stage	(9) This index is developed by considering ignitability, combustibility and sustainability. This index provides a description of the flammable properties	[17–19]
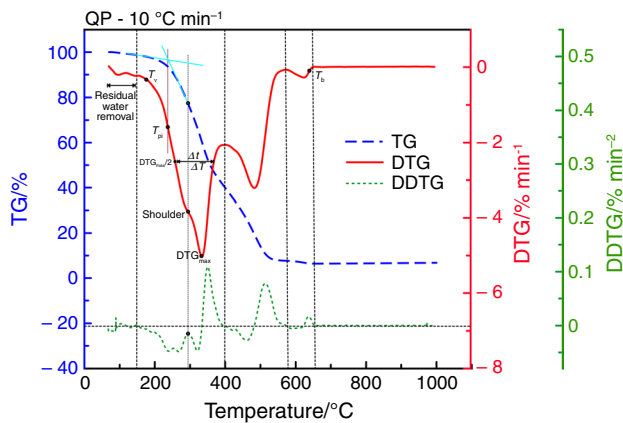
Fig. 1 Procedure for determining characteristic temperature/parameters during combustion

generalization of a logarithm. To calculate the temperature for specific cases, only the real solution is retained. The values of $E_{\alpha(\alpha)}$ and $b = \left(\left[\ln \left(A_\alpha \cdot R / E_{a(\alpha)} \right) - \ln g(\alpha) \right] \right)$ at different conversion degree are those previously calculated performing KAS method. $T(\alpha)$ is then the temperature reached by the solid at a specific conversion degree, *i.e.,* specific $E_{a(\alpha)}$ and b for the heating rate β. In Sect. "Kinetic validation", the results of temperature *vs.* conversion degree computed from Eq. 12 at different values of β are presented to ensure the reliability of the kinetic study.

Complete methodology

Based on chemical, thermal and kinetic analyses, the objective was to identify the most relevant parameters regarding the fire risk. It seemed unwise to take each parameter independently without correlating them. It was therefore necessary to develop a method of harmonization to highlight the relationships between each parameter and compare them. This method comes in two main steps. The first consists of an analytical method in which the parameters obtained serve as inputs for the calculations of the combustion indices. This step is also an opportunity to confirm the processes observed in TGA using chemical data. Then, the linear regression between combustion indices and heating rates (except for SSI, see Sect. "Combustion characteristic indices") gives a linear equation for each sample. Slopes were taken as moderate values for these indices.

The second stage of the methodology presented itself as a comprehensive study, for which a comparison of the combustion characteristic indices was analyzed and discussed for the investigated species. This stage is completed by a kinetic analysis that provides the activation energy. All the parameters allow robust classification of the selected species toward wildland fire risk management. The flow diagram of the whole methodology is presented in Fig. 2.
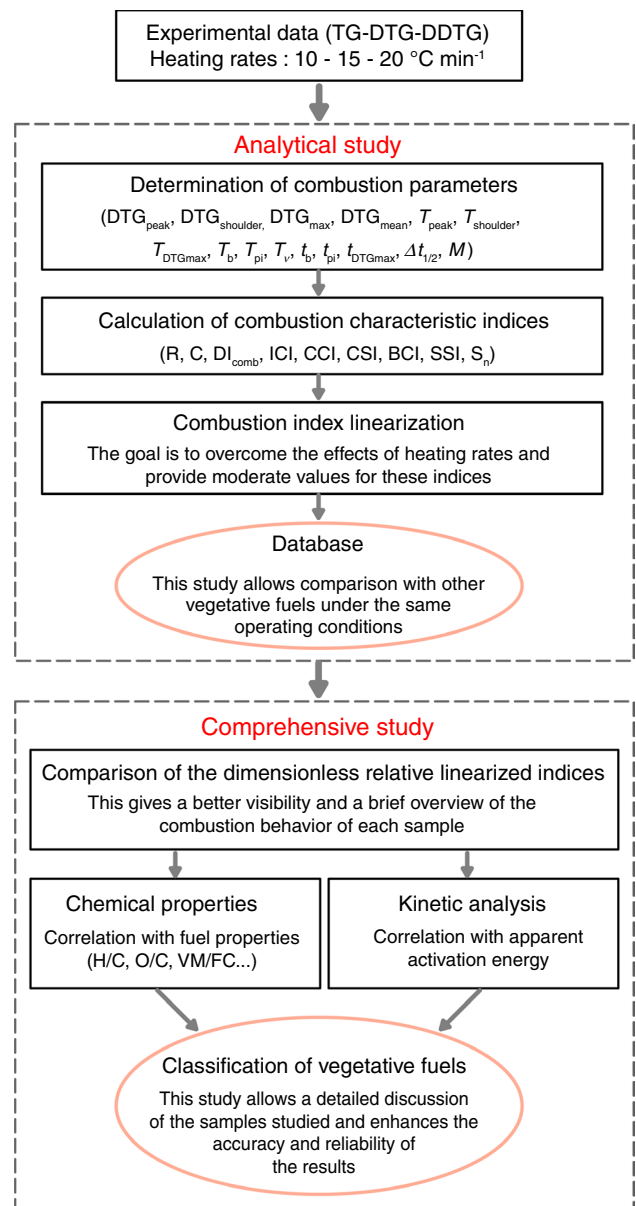

Fig. 2 Flow diagram of the methodology followed for assessing combustion characteristic indices

## Results and discussion

Characterization of vegetative fuels

Proximate and ultimate analyses were performed to characterize different plant fuels. The measured values for each sample are listed in Table 2. The results show that the tested vegetative fuels contain large amounts of volatile compounds. High levels of volatiles increase the emission rate of combustible gases, accelerating the ignition process. As a result, the fuel becomes more reactive during oxidative pyrolysis. In this case, OE may be the most reactive and

Table 2 Proximate and ultimate analysis of samples

Vegetative fuels	Proximate analysis (mass % on dry basis)			Ultimate analysis (mass % on dry ash free basis)					Energy content (MJ/kg)	
	VM	FC	Ash	C	H	N	S	O	HHV	LHV
QP	76.23	17.65	6.12	49.11	6.37	1.33	0.02	43.17	20.04	17.45
QS	80.92	16.11	2.97	49.23	6.08	1.28	0.04	43.38	19.83	17.31
OE	81.69	13.43	4.88	48.85	6.74	1.46	0.05	42.90	20.47	17.78
GSN [29, 32]	77.95	20.11	1.94	51.99	6.87	1.98	0.03	39.12	22.10	19.29

Where VM, FC, HHV and LHV are volatile matter, fixed carbon, high heating value and low heating value.
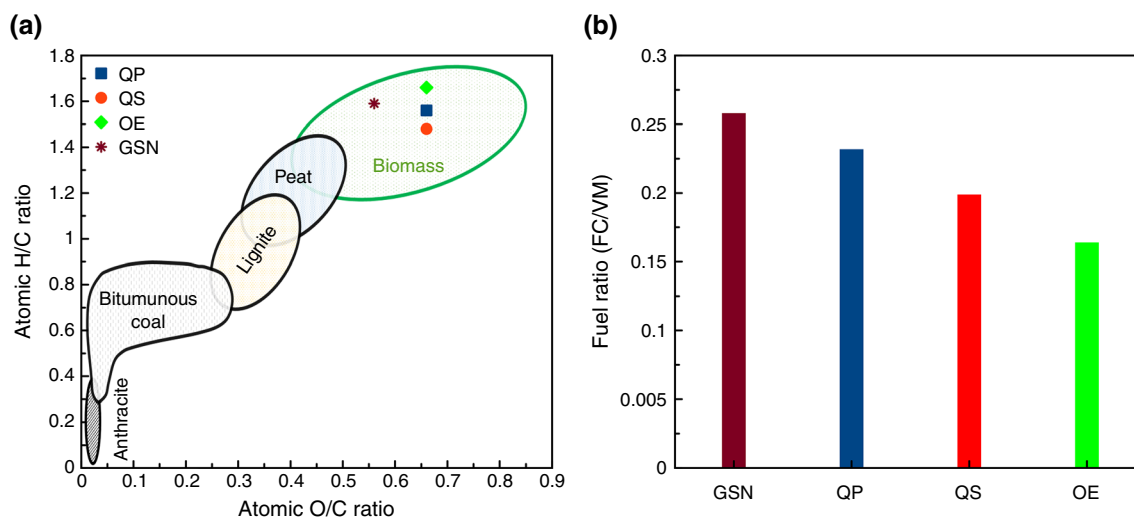
Fig. 3 Van Krevelen diagram (**a**) and fuel ratio (**b**) for the studied plant species

ignitable material compared to other samples. The QP with a higher ash content tends to produce more dust in a fire. Moreover, all samples contain relatively low nitrogen and sulfur contents. This is desirable considering NO_x and SO_2 emissions to the atmosphere. In addition, the Van Krevelen diagram (Fig. 3a) shows that all samples examined fall within the typical biomass range. The OE with higher O/C and H/C may present higher smoke and vapor losses due to oxidation excess [48]. The GSN has a higher calorific value than other samples. This is due to the higher fuel ratio (see Fig. 3b) and the lower O/C ratio and ash content of GSN. Fixed carbon contributes more to heat release than volatiles, so a higher FC/VM ratio increases the energy content of fuels [49]. Finally, the thermal decomposition behavior should be investigated to rank the materials tested according to their reactivity, ignitability and flammability indices.

Analysis of TG-DTG profiles

The TGA and derivative thermogravimetric (DTG) curves for the combustion of four plant species at three heating rates of 10, 15 and 20 °C min^{-1} are shown in Fig. 4a. DTG curves were compared with those of xylan, cellulose and lignin (in Fig. 4b) in order to identify and explain the different mechanisms of thermal decomposition. Comparisons were made based on the combustion stage and the temperature range of each component. Once the moisture is released (T < 150 °C), the combustion process at the three heating rates consists all of (1) devolatilization and (2) char oxidation. The differences in the peak positions and heights of the four samples (Fig. 4a) were mainly due to the distribution of biomass components. The three main components of vegetative fuels were hemicellulose, cellulose and lignin [50]. Volatiles are the principal products of hemicellulose and cellulose during oxidative pyrolysis, whereas char is the main product of the decomposition of lignin [51]. At the end of the combustion process (T > 680 °C), a continuous region corresponding to the non-combustible residue (ash) was observed. Table 3 summarizes detailed information about the TG-DTG properties of the investigated materials. Obviously, the heating rate affected the characteristic temperature and the mass loss rate. Heat lag and heat transfer limitations caused the reaction temperature to shift laterally to higher values with increasing heating rate [52]. A high heating rate also leads to a rapid degradation of the lignocellulosic component of the sample.

Fig. 4 **a** TG-DTG profiles of studied species at different heating rates (10, 15, and 20 °C min^{-1}) in air. **b** Typical TG-DTG curves for the main biomass component at 15 °C min^{-1}
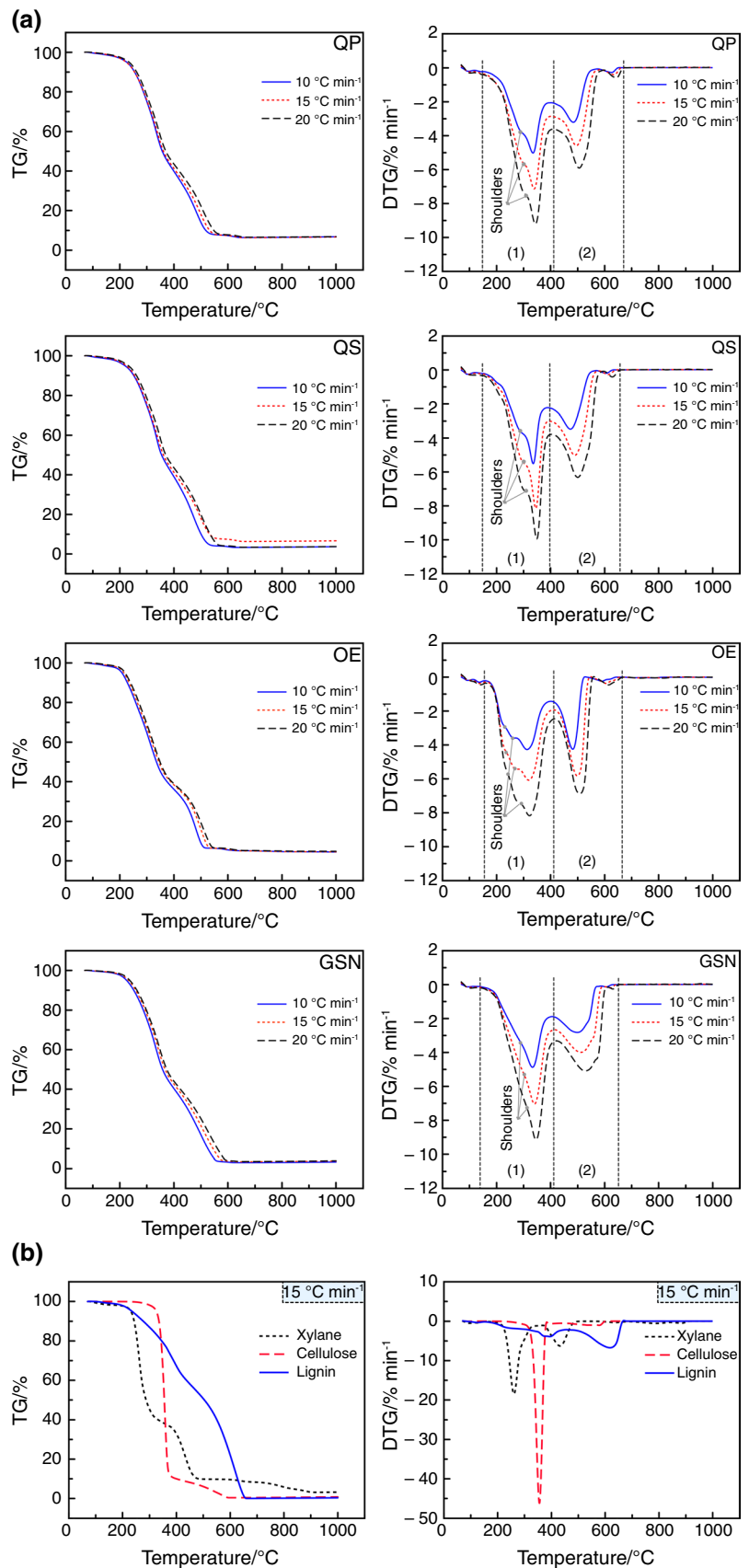
Table 3 Main TG-DTG characteristics

	HR	TR (°C) Stage 1	$R_{shoulder}$/% min^{-1}	$T_{shoulder}$ (°C)	R_{peak}/% min^{-1}	T_{peak} (°C)	TR (°C) Stage 2	R_{peak}/% min^{-1}	T_{peak} (°C)	R_{peak}/% min^{-1}	T_{peak} (°C)
QP	10	155−400	3.85	296	5.02	335	400−658	3.21	484	0.28	625
	15	145−405	5.65	301	7.14	339	405−666	4.59	496	0.41	635
	20	145−410	7.46	307	9.2	344	410−680	5.91	506	0.59	643
QS	10	150−390	3.73	296	5.51	336	390−635	3.47	473	0.2	605
	15	145−400	5.51	303	8.14	345	400−650	5.01	490	0.27	613
	20	145−405	7.17	308	9.94	349	405−665	6.31	501	0.41	628
OE	10	155−405	2.92	230	4.27	313	405−650	4.25	482	0.24	589
			3.59	268							
	15	160−410	4.43	236	6.08	319	410−660	5.82	499	0.37	605
			5.44	274							
	20	160−415	5.61	240	8.17	322	415−670	6.88	508	0.46	614
			7.44	286							
GSN	10	140−407	3.35	287	4.87	333	407−635	2.82	499	0.13	606
	15	140−415	5.17	298	7.04	341	415−650	3.99	513	0.19	620
	20	145−422	6.96	306	9.14	346	422−660	5.09	527	0.26	630

Figure 4b clearly shows that xylan was the most degradable, followed by cellulose, while lignin was the least degradable (high decomposition temperature). It appears that the main DTG peaks associated with xylan and cellulose degradation (Fig. 4b) coincide with the shoulders and DTG peaks detected in stage 1 of Fig. 4a. Thus, the degradation of hemicellulose was responsible for the shoulder, and the peak appeared due to the degradation of cellulose. The same behavior was reported by Liu et al. [11]. Similarly, the main peak of degradation of lignin corresponds to the char oxidation zone (stage 2). In addition, the mass loss rate of lignin was less than that of cellulose and xylan. This is consistent with the results of the samples examined, since the rate of mass loss during char oxidation was smaller than that during devolatilization. Finally, the last combustible lignin fraction was oxidized at high temperatures (530–680 °C). This was due to the high thermal stability and the presence of aromatic compounds, which required high temperatures to achieve full oxidation [12].

Comparing the first stages of thermal degradation of the four samples, it can be observed that the devolatilization stage initiated earlier for OE. This may be explained by the more volatile content of OE in comparison with QP, QS and GSN (Table 2). In addition, the peak oxidation temperature of QS-char was lower than that of other samples (see Table. 3). This can reflect the potentially high reactivity of QS-char and the high burnout properties of this sample. Furthermore, char combustion (stage 2) of all samples was slower compared to devolatilization (stage 1). For GSN, the char combustion peak shifts to higher temperatures (Table 3). This can be explained by the highest carbon content and fixed carbon in the material. Nevertheless, the highest DTG$_{peak}$ of char burning is obtained for OE due to the lowest fixed carbon.

Analytical study of the combustion characteristic indices

Vegetative fuels are highly reactive substances. These materials, particularly dead surface combustibles that accumulate on the forest floor, may present a significant fire hazard. For this reason, ranking the relative ignition risk of these species can assist in forest fire management planning. Following the procedure described above in Sect. "Combustion characteristic indices", Fig. S2 (a) shows the linearization plots of the identified characteristic temperatures and their mass loss rate (DTG) of the samples studied. In this case, T_v, T_{pi}, $T_{shoulder}$ (the largest shoulder, particularly in OE), and T_{peak} were selected. DTG values were linearly related to the selected temperature ($R^2 > 0.9$ for all heating rates). The relation between the slopes obtained in Fig. S2 (a) and the heating rates is illustrated in Fig. S2 (b). The R^2 for all samples was greater than 0.98, indicating a high degree of
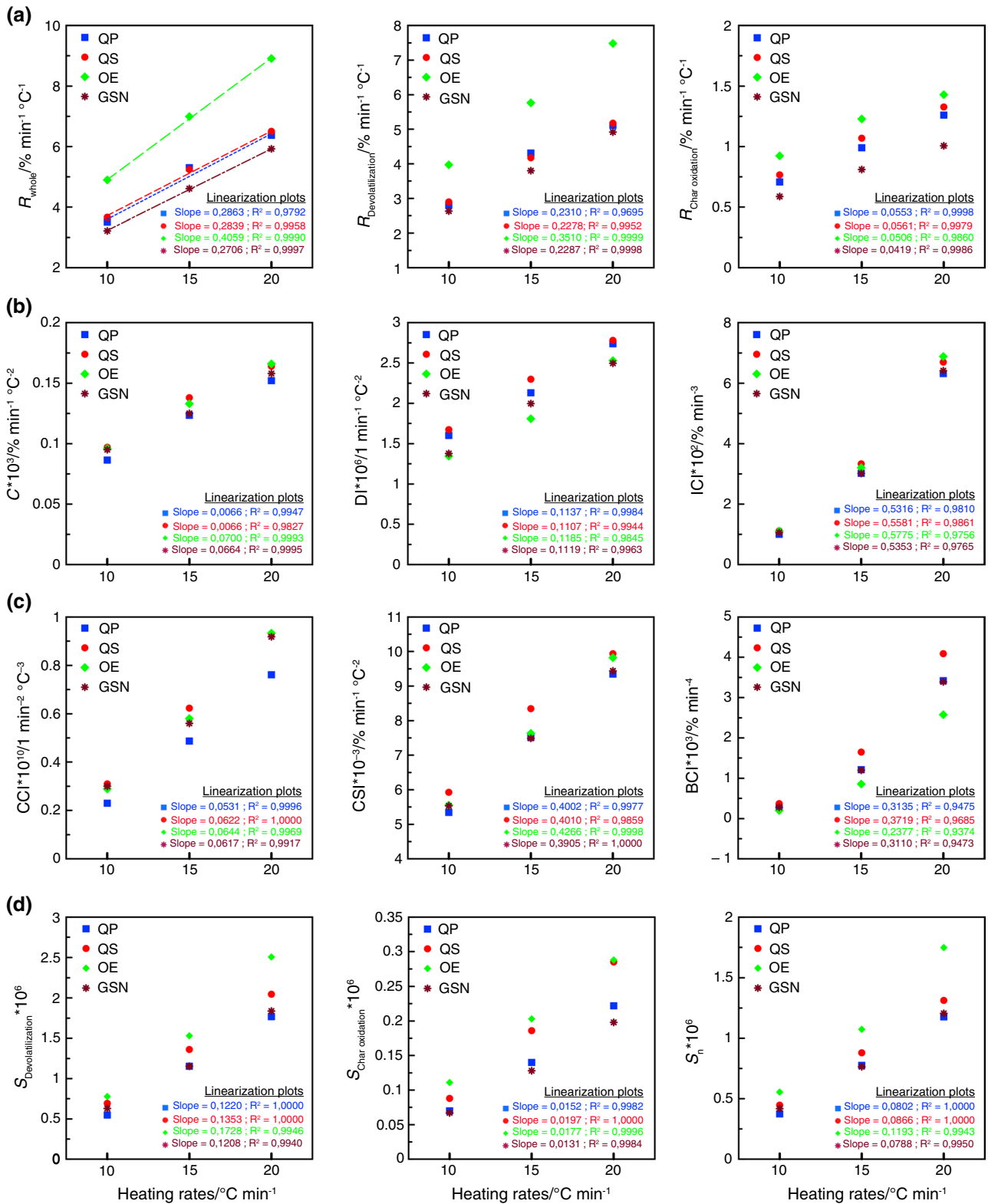
Fig. 5 The relationship between combustion indices and heating rates: **a** reactivity, **b** ignitability, **c** combustibility and burnout and **d** integrated flammability
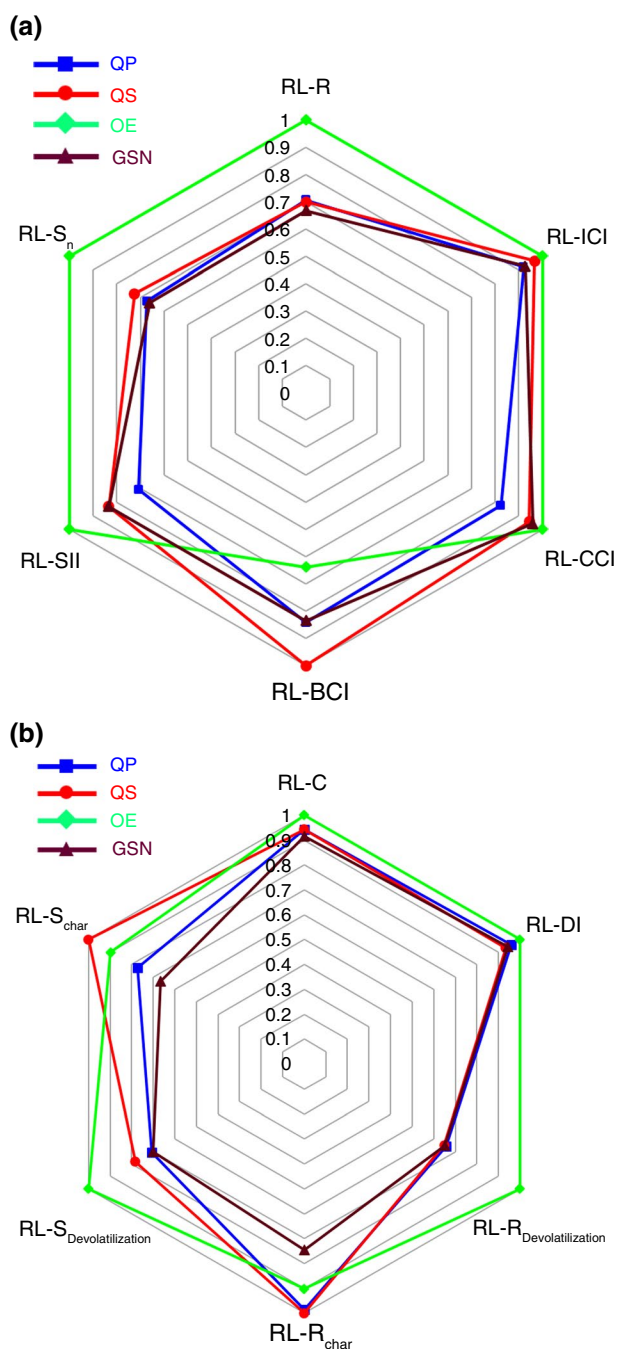
(a)

(b)

Fig. 6 Radar charts of the global (**a**) and local (**b**) RL indices for the studied forest species

confidence in the calculation of the SII. Using the slopes in Fig. S2 (b), the SII values were 0.0017, 0.0020, 0.0024 and 0.0020 for QP, QS, OE and GSN, respectively. Therefore, the ignition potential of OE was slightly higher than that of other samples and could be easily burned. Extreme caution should be taken, especially in the summer and after olive harvesting, as the surface dead OE fuel that accumulates on the forest soil can easily ignite.

The other combustion indices of reactivity (R, $R_{Devolatilization}$ and $R_{char\ oxidation}$), ignitability (C, DI and ICI), combustibility (CCI, CSI), burnout (BCI) and integrated flammability (S_n, $S_{Devolatilization}$ and $S_{char\ oxidation}$) were calculated. These indices depend on TG-DTG parameters and characteristic temperatures (listed in Table S1), which in turn are not fundamental properties of the fuel [53]. Table S1 shows that various characteristic temperatures and DTG values shift to a higher range with increasing heating rate. Figure 5a–d clearly shows that all combustion indices also shift to higher values as the heating rate increases, demonstrating that the higher heating rates can enhance the thermal reactivity, flammability, and combustibility of the samples. The linearized curves shown in Fig. 5a–d depict the relationship between the combustion indices and the three different heating rates.

By plotting the curves in this way, it is possible to observe how the combustion indices change as the heating rate increases. This can be useful for understanding the behavior of the materials being studied and predicting how they will behave under different conditions. Each combustion index of the studied species increases proportionally with heating rate. A good linearity was observed with all linear correlation coefficients (R^2) greater than 0.9. The resulting slopes will be used to accurately compare the combustion behavior of the investigated samples.

Comprehensive study of the combustion characteristic indices

Radar charts were used to compare the most relevant combustion indices based on the slopes obtained in Fig. 5. In this section, these slopes were called relative linearized (RL) indices. The results are presented in Fig. 6 in the form of global (a) and local (b) RL indices. All parameters were dimensionless for better visibility. This gives a brief overview of the combustion behavior of each sample.

Here, as the same behavior was observed in the RL-ICI and RL-CSI rankings, only RL-ICI was retained for comparison purposes. From Fig. 6a, all OE indices, apart from RL-BCI, were higher than those of QP, QS and GSN, indicating that OE was the most reactive, ignitable and combustible material. These differences are primarily related to the chemical properties of the samples. During devolatilization, the higher volatile component of OE (see Table 2) and its early release, along with the higher H/C ratio (Fig. 3), contributed to a faster heat release during combustion. As a result, reactivity, ignition and combustion performances were higher in this sample. This behavior was also reported by García Torrent et al. [25], confirming that a higher propensity to self-ignite was observed in biomasses with a higher H/C ratio. Figure 6b also proves these findings by analyzing the local characteristics of the RL indices (C, DI,
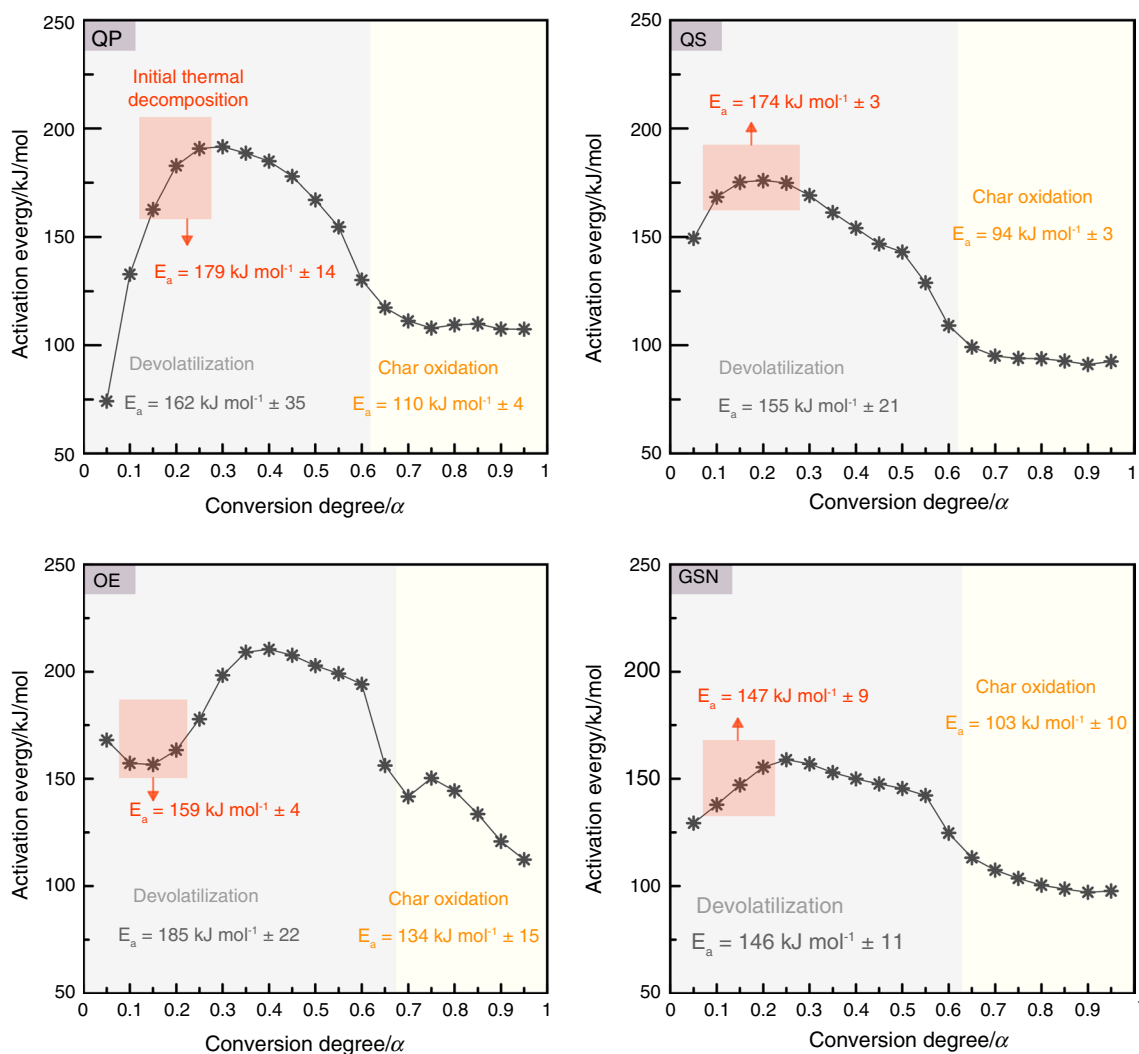
Fig. 7 Changes of apparent activation energy with the conversion degree

S-R$_{\text{Devolatilization}}$ and S$_{\text{Devolatilization}}$) of the devolatilization stage. This figure shows higher oxidative pyrolysis performances for the OE sample. Moreover, the lower RL-BCI of OE implies a lower burning reactivity of fixed carbon. This is reflected by the low reactivity of OE char, which rank immediately before GSN (Fig. 6b). In addition, GSN with a low O/C ratio has the lowest reactivity and flammability (RL-R$_{\text{char}}$ and RL-S$_{\text{char}}$, respectively) during the oxidation stage of char. This can be explained by the fact that the low oxygen content of GSN reduces the rates of devolatilization and char oxidation. Furthermore, the near combustion index values for QP, QS and OE during devolatilization could be linked to the equal O/C ratios obtained for these samples. The same was also the case for the whole process in terms of RL-R, RL-ICI and RL-S$_n$. On the other hand, we can generally see from Fig. 6a that the RL indices of QP show the narrowest hexagon. This may be attributed to the high

ash content (6.12 mass%) of QP, which can affect oxygen diffusion and heat transfer [54].

Kinetic analysis

Activation energy determination

Activation energy (E) means the minimum amount of energy needed to initiate a chemical reaction. Based on the KAS method, the apparent activation energy (E$_a$) was calculated at different conversion degrees (α), as shown in Fig. 7. The results showed higher R^2 (except for QP with α = 0.05–0.15) and provided reliable values for E$_a$ (see linearized plot in Fig. S3).

A low E$_a$-value may indicate an early initiation of the reaction, but risk assessment based only on E$_a$ has not been shown to be valid for biomass [25]. For this reason, the discussion of kinetic analysis of selected plant species will be
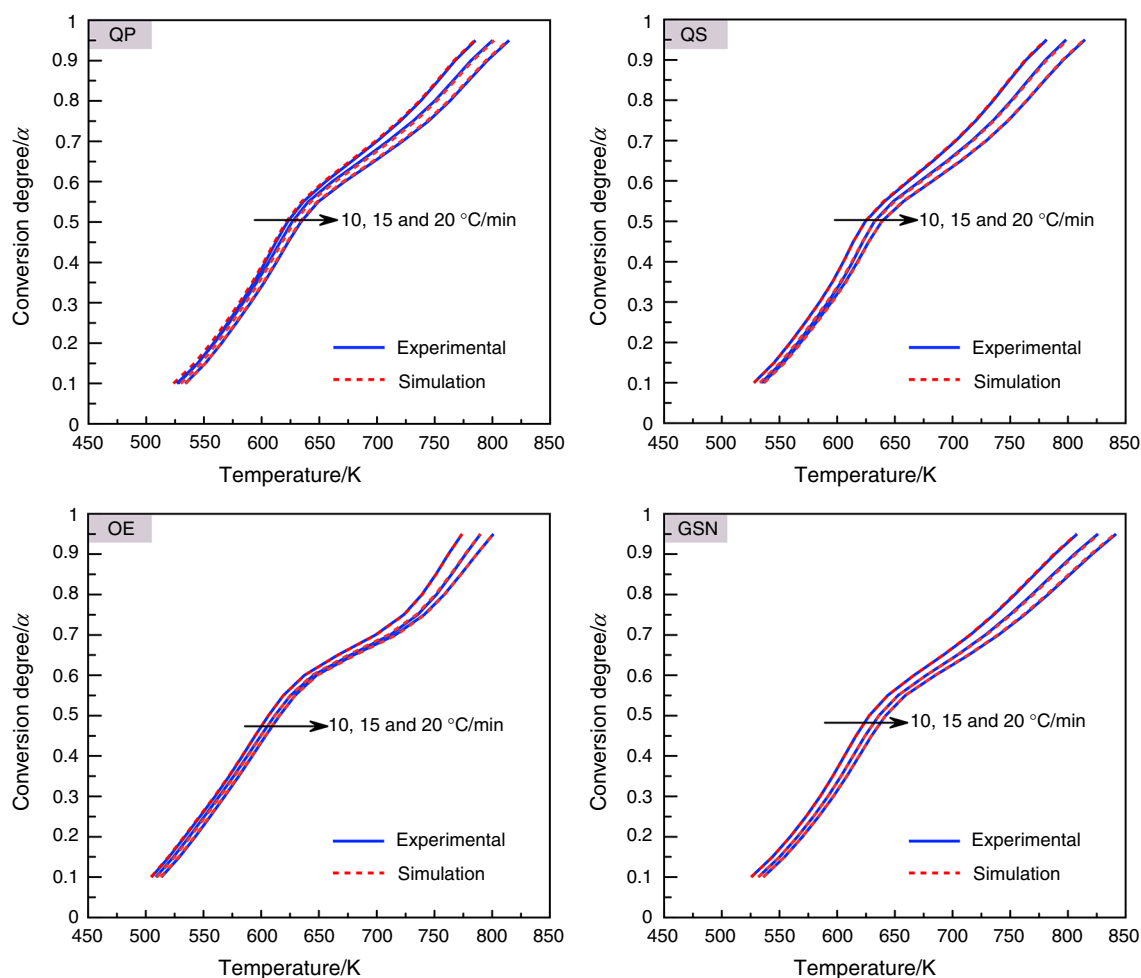
Fig. 8 Experimental (line) and simulated (dashed line) curves using the kinetic data calculated from KAS method

related to their chemical properties and combustion indices. The average E_a values associated with initial thermal decomposition (red square), devolatilization and char oxidation are listed in Fig. 7. In the early stages of combustion ($\alpha = 0.1$ to 0.25), E_a was found in the following order of magnitude: E_a (QP) > E_a (QS) > E_a (OE) > E_a (GSN). At this stage, GSN and OE have much lower E_a, implying that less energy is required to initiate hemicellulose degradation in these two species than for QP and QS. In addition, OE starts the thermal decomposition with a decrease in E_a. This indicates that the energy barrier prior to ignition was weak. Compared to GSN, OE has the highest H/C ratio and the lowest fuel ratio (FC/VM), leading to severe volatile emissions. This may explain the delay in ignition of GSN (longer reaction time and slower combustion rate) despite the low E_a value (see Fig. 6a). As a result, we found that the rankings obtained by RL-SII (OE > GSN ≥ QS > QP) and RL-CCI (OE > GSN > QS > QP) complied with the above results and explanations. In addition, the E_a variation trend with α for QP and QS was the same. QP and QS have the nearest

E_a values, which can reflect similarities in lignocellulosic composition. After devolatilization ($\alpha > 0.65$), the E_a of QP, QS and GSN were significantly reduced in the oxidation stage of char. However, E_a for oxidation of OE char shows an increase at ($\alpha = 0.75$) and then, decreases gradually. In this case, the energy barrier to be overcome during char oxidation was more important for OE than for other samples. This means a slower OE response and a great delay in fixed carbon combustion. This behavior fully supports the lowest burnout performance (RL-BCI) of the OE sample shown in Fig. 6a.

Kinetic validation

Eq. 12 allows the calculation of $E_{a(\alpha)}$ and b for the whole process at 10, 15 and 20 °C min^{-1}. These values can be used to accurately describe the dependence of conversion degree on temperature for different heating rates. The numerical results were plotted and compared to those of the experiments in Fig. 8.

As shown in Fig. 8, the simulated plots were consistent with the experimental ones. These results were supported by good correlation coefficients of the slopes obtained with the KAS method, thereby ensuring reliable kinetic parameters.

Closing remarks

An in-depth analysis of the above results enables us to conclude that the chemical properties (particularly the FC/VM and H/C ratios, the ash content, etc.) and the apparent activation energy have an acceptable correlation with the combustion indices.

The study investigated the burning characteristics of different plant species using various combustion indices, including apparent activation energy, to understand their fire risk and combustion activity. The results showed that OE had a higher level of fire risk and combustion activity compared to GSN, QP, and QS.

However, the main objective was to provide a simple analytical tool to compare the spontaneous combustion of various plant species. The study acknowledged the difficulty in reaching a global consensus for selecting relevant combustion indices for fire risk assessment due to the complex multiphase reactions of these species. Overall, this work provides useful information on the burning characteristics of different plant species and their potential fire risk.

In the present work, further analysis of Fig. 6a shows a notable assessment of the studied plant species for RL-R, RL-BCI, RL-SII and RL-Sn. Otherwise, the rankings of the other RL indices (ICI, CCI, CSI, C and DI) were very close and sometimes inseparable (in the case of RL-DI and RL-C). This behavior restricts the use of these indices to provide reliable classification of plant species. Based on the above results and observations, we believe that RL-SII and RL-Sn can provide a precise classification of the risk of spontaneous ignition/combustion. In addition, RL-R can be used as a preliminary index to estimate the pyrolysis activity, and RL-BCI can be used to estimate the char burning activity. From a kinetic analysis point of view, the result was consistent with classification by RL indices. Among the samples investigated, the high stability of GSN was visualized by the low amplitude level of fluctuations in E_a. This means that once ignited, the GSN may react quickly and burn out. Similarly, the reason for the lower RL-BCI in OE was visualized in the slight increase in E_a values at $\alpha = 0.75$ due to the reactivation of char burning. Finally, the presented kinetic data are also important for modeling wildland fires.

Conclusions

Four plant species were evaluated using proximate and ultimate data, thermal decomposition behavior, combustion characteristic indices and kinetic analysis. The main combustion process was controlled by the devolatilization step, which consumed about 57–62% of the mass loss. Thermal degradation behavior was evaluated from the TG-DTG curves, providing information on reactivity, spontaneous ignition, flammability/combustibility and burnout. Except for RL-BCI, all other RL indices were found to be significantly higher in OE than in other samples. The relevant RL indices of the devolatilization stage show the same behavior. This made OE more reactive, easier to burn and hence, more prone to fire. Furthermore, the lower RL-BCI of OE indicated a slow fixed carbon burning reaction. This was also evident considering the associated char oxidation indices, where OE was underclassified in comparison with QP and QS. Meanwhile, the apparent activation energy (E_a) was determined using the FWO and KAS methods. In the early stages of combustion ($\alpha \approx 0.1 - 0.25$), the average E_a values for GSN and OE were lower than QP and QS. Thus, less energy was required for GSN and OE to begin the combustion process. The higher ignition performance of OE, compared to GSN, was related to the higher H/C ratio and the early decrease in E_a at the onset of combustion ($\alpha = 0.05 - 0.15$). Finally, the RL-SII and RL-S$_n$ indices were selected as appropriate parameters for classifying spontaneous combustion risk. Further work should address other plant species in order to offer a comprehensive database of fuels to support fire management. Moreover, the proposed methodology herein can also be useful for other applications, such as the safe storage of biofuels or the use of these biomaterials as a source of energy. For example, GSN with a lower activation energy, a low ash content and a high calorific value may be good candidates for direct combustion. OE with high volatile compounds, a high H/C ratio and relatively low fixed carbon content point to a high potential for anaerobic digestion.

Author contributions YR contributed to conceptualization, methodology, validation, investigation, formal analysis, writing—original draft, writing—review & editing, visualization. VLC contributed to conceptualization, methodology, validation, formal analysis, resources, writing—review & editing, visualization, project administration. DC contributed to conceptualization, methodology, validation, investigation, resources, writing—review & editing, visualization, project administration. JF contributed to investigation, formal analysis, validation. JLR

contributed to investigation, formal analysis, validation. EL contributed to investigation, formal analysis, validation.

References

1. Jolly WM, Cochrane MA, Freeborn PH, Holden ZA, Brown TJ, Williamson GJ, Bowman DMJS. Climate-induced variations in global wildfire danger from 1979 to 2013. Nat Commun. 2015;6:1–11.

2. González Martínez M, Dupont C, da Silva PD, Míguez-Rodríguez L, Grateau M, Thiéry S, Tamminen T, Meyer XM, Gourdon C. Assessing the suitability of recovering shrub biowaste involved in wildland fires in the South of Europe through torrefaction mobile units. J Environ Manage. 2019;236:551–60.

3. Scott AC, Bowman DM, Bond WJ, Pyne SJ, Alexander ME. Fire on earth: an introduction. New York: Wiley; 2014.

4. Abbas D, Current D, Ryans M, Taff S, Hoganson H, Brooks KN. Harvesting forest biomass for energy - an alternative to conventional fuel treatments: trials in the Superior National Forest, USA. Biomass Bioenerg. 2011;35:4557–64.

5. Singh P. Potential of pine needle biomass as an alternative fuel to mitigate forest fire in Uttarakhand Himalayas - a review. J Agric Eng. 2022;58:192–203.

6. Jones JM, Saddawi A, Dooley B, Mitchell EJS, Werner J, Waldron DJ, Weatherston S, Williams A. Low temperature ignition of biomass. Fuel Process Technol. 2015;134:372–7.

7. Armakan S, Civan M, Yurdakul S. Determining co-combustion characteristics, kinetics and synergy behaviors of raw and torrefied forms of two distinct types of biomass and their blends with lignite. J Therm Anal Calorim. 2022;147:12855–69.

8. Meena MK, Anand S, Ojha DK. Interdependency of pyrolysis and combustion: a case study for lignocellulosic biomass. J Therm Anal Calorim. 2023;148:5509–19.

9. Wnorowska J, Ciukaj S, Kalisz S. Thermogravimetric analysis of solid biofuels with additive under air atmosphere. Energies. 2021;14(8):2257.

10. Paniagua Bermejo S, Prado-Guerra A, García Pérez AI, Calvo Prieto LF. Study of quinoa plant residues as a way to produce energy through thermogravimetric analysis and indexes estimation. Renew Energy. 2020;146:2224–33.

11. Liu C, Liu J, Evrendilek F, Xie W, Kuo J, Buyukada M. Bioenergy and emission characterizations of catalytic combustion and pyrolysis of litchi peels via TG-FTIR-MS and Py-GC/MS. Renew Energy. 2020;148:1074–93.

12. Zhang Y, Kang L, Li H, Huang X, Liu X, Guo L, et al. Characterization of moxa floss combustion by TG/DSC, TG-FTIR and IR. Bioresour Technol. 2019;288.

13. El-Sayed SA, Ismail MA, Mostafa ME. Thermal decomposition and combustion characteristics of biomass materials using TG/DTG at different high heating rates and sizes in the air. Environ Prog Sustain Energy. 2019;38:1–14.

14. Wang Q, Wang G, Zhang J, Lee JY, Wang H, Wang C. Combustion behaviors and kinetics analysis of coal, biomass and plastic. Thermochim Acta. 2018;669:140–8.

15. Song Y, Liu J, Evrendilek F, Kuo J, Buyukada M. Combustion behaviors of Pteris vittata using thermogravimetric, kinetic, emission and optimization analyses. J Clean Prod. 2019;237: 117772.

16. Liu X, Chen M, Yu D. Oxygen enriched co-combustion characteristics of herbaceous biomass and bituminous coal. Thermochim Acta. 2013;569:17–24.

17. Zhang Z, Zhang H, Zhou D. Flammability characterisation of grassland species of Songhua Jiang-Nen Jiang Plain (China) using thermal analysis. Fire Saf J. 2011;46:283–8.

18. Anderson HE. Forest fuel ignitibility. Fire Technol. 1970;6:312–9.

19. Liodakis S, Kakardakis T. Measuring the particle flammability of forest species from wildland/urban interface (WUI) near athens by thermal analysis. In: 2006 1st international symposium environment identities Mediterranean area, ISEIM. 2006;24–8

20. Xie T, Wei R, Wang Z, Wang J. Comparative analysis of thermal oxidative decomposition and fire characteristics for different straw powders via thermogravimetry and cone calorimetry. Process Saf Environ Prot. 2020;134:121–30.

21. Manić N, Janković B, Stojiljković D, Radojević M, Somoza BC, Medić L. Self-ignition potential assessment for different biomass feedstocks based on the dynamic thermal analysis. Clean Eng Technol. 2021;2.

22. Kumar Mohalik N, Mandal S, Kumar Ray S, Mobin Khan A, Mishra D, Krishna PJ. TGA/DSC study to characterise and classify coal seams conforming to susceptibility towards spontaneous combustion. Int J Min Sci Technol. 2022;32:75–88.

23. Shu Y, Zhang J, Li W, Zhao P, Zhang Q, Zhou M. Thermogravimetric analysis of the pyrolysis and combustion kinetics of surface dead combustibles in the Daxing'an Mountains. PLoS ONE. 2021;16:1–16.

24. Liu L, Pang Y, Lv D, Wang K, Wang Y. Thermal and kinetic analyzing of pyrolysis and combustion of self-heating biomass particles. Process Saf Environ Prot. 2021;151:39–50.

25. García Torrent J, Ramírez-Gómez Á, Fernandez-Anez N, Medic Pejic L, Tascón A. Influence of the composition of solid biomass in the flammability and susceptibility to spontaneous combustion. Fuel. 2016;184:503–11.

26. Mandal S, Mohalik NK, Ray SK, Khan AM, Mishra D, Pandey JK. A comparative kinetic study between TGA & DSC techniques using model-free and model-based analyses to assess spontaneous combustion propensity of Indian coals. Process Saf Environ Prot. 2022;159:1113–26.

27. Jia J, Huang R, Wang Y. Study on the combustion characteristics of mountain forest vegetation. Forests. 2022;13.

28. Fayad J, Morandini F, Accary G, Chatelon FJ, Wandon C, Burglin A, Rossi L, Marcelli T, Cancellieri D, Cancellieri V, Morvan D, Meradji S, Pieri A, Planelles G, Costantini R, Briot P, Rossi JL. A study of two high intensity fires across corsican shrubland. Atmosphere. 2023;14:1–21.

29. Rahib Y, Leroy-Cancellieri V, Cancellieri D, Quilichini Y. Fire hazard analysis of Mediterranean Genista Salzmannii: pyrolysis and kinetic characterization. J Anal Appl Pyrolysis. 2022;168.

30. Loo S V and Koppejan J. The handbook of biomass combustion and co-firing. Earthscan 2008. pp. 7–14.

31. Yang J, Chen H, Zhao W, Zhou J. Combustion kinetics and emission characteristics of peat by using TG-FTIR technique. J Therm Anal Calorim. 2016;124:519–28.

32. Rahib Y, Leroy-Cancellieri V, Cancellieri D, Awad C, Rossi J-L. Comprehensive characterization of pyrolysis and combustion of genista salzmannii needles (GSN) for fire hazard analysis. In: Advances in forest fire research, Viegas DX, Ribeiro LM, editors. 2022. 1430–36

33. Sanchez ME, Otero M, Gómez X, Morán A. Thermogravimetric kinetic analysis of the combustion of biowastes. Renew Energy. 2009;34:1622–7.

34. Rahib Y, Sarh B, Chaoufi J, Bonnamy S, Elorf A. Physicochemical and thermal analysis of argan fruit residues (AFRs) as a new local biomass for bioenergy production. J Therm Anal Calorim. 2021;145:2405–16.

35. Rahib Y, Elorf A, Sarh B, Bonnamy S, Chaoufi J, Ezahri M. Experimental analysis on thermal characteristics of Argan nut shell (ANS) biomass as a green energy resource. Int J Renew Energy Res. 2019;9:1606–16015.

36. Reis JS, Araujo RO, Lima VMR, Queiroz LS, da Costa CEF, Pardauil JJR, Chaar JS, Filho GNR, de Souza LKC. Combustion properties of potential Amazon biomass waste for use as fuel. J Therm Anal Calorim. 2019;138:3535–9.

37. Li J, Hu J, Wang T, Gan J, Xie J, Shui Y, Liu J, Xue Y. Thermogravimetric analysis of the co-combustion of residual petrochemical sludge and municipal sewage sludge. Thermochim Acta. 2019;673:60–7.

38. Paniagua S, Calvo LF, Escapa C, Coimbra RN, Otero M, García AI. Chlorella sorokiniana thermogravimetric analysis and combustion characteristic indexes estimation. J Therm Anal Calorim. 2018;131:3139–49.

39. Yi B, Chen M, Gao Y, Cao C, Wei Q, Zhang Z, Li L. Investigation on the co-combustion characteristics of multiple biomass and coal under O2/CO2 condition and the interaction between different biomass. J Environ Manage. 2023;325: 116498.

40. Huang C, Yu C, Wang G, Zhang J, Ning X, Wang C. Comparison of structural characteristics and combustibility analysis about hydrochar and pyrochar. J Therm Anal Calorim. 2022;147:10509–23.

41. Yang Y, Lu X, Wang Q. Investigation on the co-combustion of low calorific oil shale and its semi-coke by using thermogravimetric analysis. Energy Convers Manag. 2017;136:99–107.

42. Vamvuka D, El Chatib N, Sfakiotakis S. Measurements of ignition point and combustion characteristics of biomass fuels and their blends with lignite. Proc Eur Combust Meet. 2011;2015:95.

43. Ahn S, Choi G, Kim D. The effect of wood biomass blending with pulverized coal on combustion characteristics under oxy-fuel condition. Biomass Bioenerg. 2014;71:144–54.

44. Vyazovkin S, Burnham AK, Criado JM, Pérez-Maqueda LA, Popescu C, Sbirrazzuoli N. ICTAC kinetics committee recommendations for performing kinetic computations on thermal analysis data. Thermochim Acta. 2011;520:1–19.

45. Ben Abdallah A, Ben Hassen Trabelsi A, Navarro MV, Veses A, García T, Mihoubi D. Pyrolysis of tea and coffee wastes: effect of physicochemical properties on kinetic and thermodynamic characteristics. J Therm Anal Calorim. 2023;148:2501–15.

46. Wilk M, Magdziarz A, Gajek M, Zajemska M, Jayaraman K, Gokalp I. Combustion and kinetic parameters estimation of torrefied pine, acacia and Miscanthus giganteus using experimental and modelling techniques. Bioresour Technol. 2017;243:304–14.

47. Leroy V, Cancellieri D, Leoni E, Rossi JL. Kinetic study of forest fuels by TGA: model-free kinetic approach for the prediction of phenomena. Thermochim Acta. 2010;497:1–6.

48. Wu KT, Tsai CJ, Chen CS, Chen HW. The characteristics of torrefied microalgae. Appl Energy. 2012;100:52–7.

49. Du SW, Chen WH, Lucas JA. Pretreatment of biomass by torrefaction and carbonization for coal blend used in pulverized coal injection. Bioresour Technol. 2014;161:333–9.

50. Mukhopadhyay S, Sarkar P, Masto RE, Singh AK, Singh PK. Investigation on the combustion characteristics of different plant parts of Cassia siamea by DSC-TGA. J Therm Anal Calorim. 2022;147:3469–81.

51. Deng S, Wang X, Tan H, Mikulčić H, Yang F, Li Z, et al. Thermogravimetric study on the co-combustion characteristics of oily sludge with plant biomass. Thermochim Acta. 2016;633:69–76.

52. Xu F, Wang B, Yang D, Hao J, Qiao Y, Tian Y. Thermal degradation of typical plastics under high heating rate conditions by TG-FTIR: pyrolysis behaviors and kinetic analysis. Energy Convers Manag. 2018;171:1106–15.

53. Tian B, Qiao YY, Tian YY, Liu Q. Investigation on the effect of particle size and heating rate on pyrolysis characteristics of a bituminous coal by TG-FTIR. J Anal Appl Pyrolysis. 2016;121:376–86.

54. Mureddu M, Dessì F, Orsini A, Ferrara F, Pettinau A. Air- and oxygen-blown characterization of coal and biomass by thermogravimetric analysis. Fuel. 2018;212:626–37.